EUROPEAN LABORATORY FOR PARTICLE PHYSICS

CERN-SPSC/97-21
SPSC/I 216
October 10, 1997

LETTER OF INTENT

SEARCH FOR $\nu_\mu \rightarrow \nu_e$ OSCILLATION AT THE CERN PS

N. Armenise, F. Cassol, M. G. Catanesi, M. T. Muciaccia, E. Radicioni, S. Simone, L. Vivolo:
Università di Bari and INFN, Bari, Italy

M. Van der Donckt[1], B. Van de Vyver[2], P. Vilain[3], G. Wilquet[3]:
IIHE (ULB-VUB), Brussels, Belgium

B. Saitta:
Università di Cagliari and INFN, Cagliari, Italy

L. La Rotonda:
Università della Calabria and INFN, Cosenza, Italy

E. Di Capua, P. Zucchelli:
Università di Ferrara and INFN, Ferrara, Italy

J. Brunner, M. Litmaath, L. Ludovici[4], S. Ricciardi, E. Tsesmelis:
CERN, Geneva, Switzerland

G. Atoyan, N. Goloubev, M. Kirsanov, A. Scassirskaj:
Institute for Nuclear Research, Moscow, Russia

V. Palladino:
Università Federico II and INFN, Naples, Italy

M. Baldo-Ceolin, D. Gibin, A. Guglielmi, M. Laveder, M. Mezzetto:
Università di Padova and INFN, Padova, Italy

D. De Pedis, U. Dore, A. Frenkel, P. F. Loverre, A. Maslennikov, R. Santacesaria:
Università La Sapienza and INFN, Rome, Italy

The following institutes expressed their interest:

METU (Ankara), Harvard (Cambridge, MA)
UCL (Louvain-la-Neuve), ITEP (Moscow)

---

[1]Fonds pour la Formation a la Recherche dans l'Industrie et dans l'Agriculture
[2]National Fonds voor Wetenschappelijk Onderzoek
[3]Fonds National de la Recherche Scientifique
[4]On leave of absence from Università 'La Sapienza' and INFN, Rome, Italy

1 Introduction

Experimental evidence from several sources suggests with a different degree of confidence that neutrino oscillations may take place. Indeed, the deficit of solar neutrinos relative to the expectations of the standard solar model and the apparent deficit of ν_μ produced by cosmic ray interactions in the atmosphere find a natural, although not unique, explanation in that phenomenon. Furthermore there is a claim by the LSND collaboration of a direct observation of $\bar{\nu}_\mu \rightarrow \bar{\nu}_e$ and of $\nu_\mu \rightarrow \nu_e$ transitions for neutrinos from pion decays, at rest and in flight [1, 2].

The most likely values for neutrino mass differences and mixing angles from these experiments are shown in fig. 1, together with upper limits from other experiments.

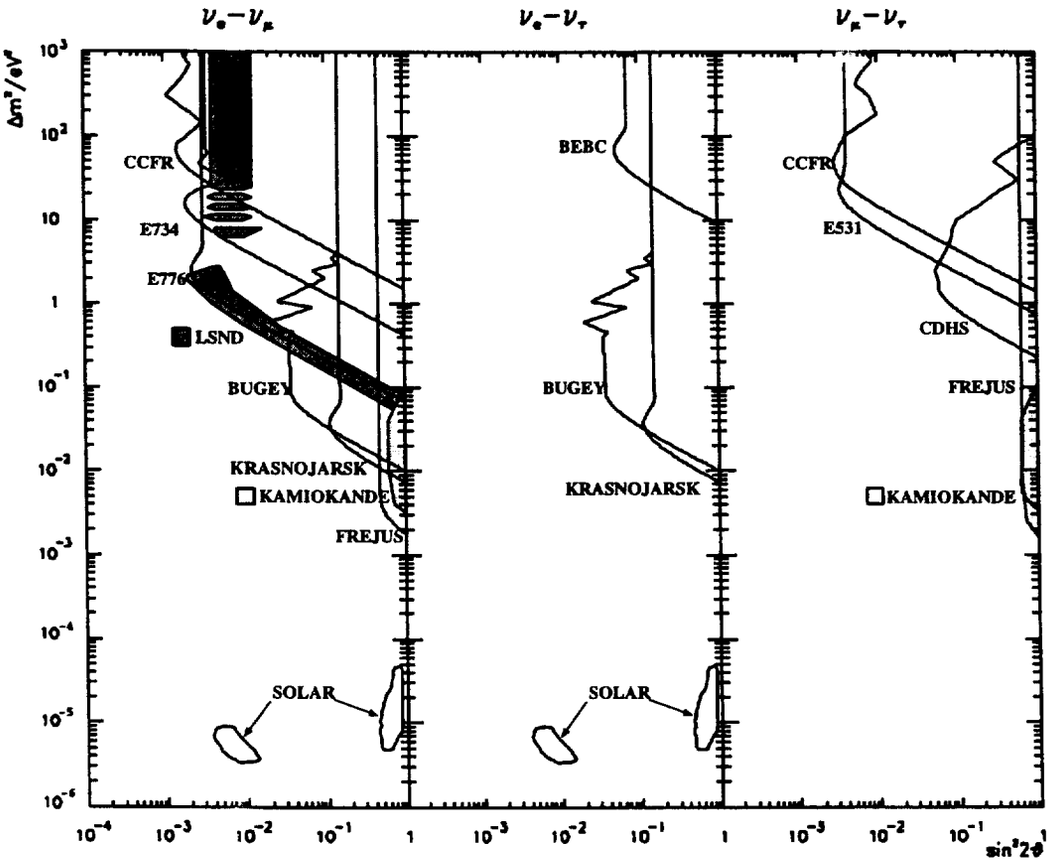

Figure 1: Status of oscillation claims and limits.

There exist a variety of models that appear to be able to accommodate virtually every pattern of neutrino masses [3, 4, 5, 6]. The rapid changes in the preferred views - from the seesaw mechanism to the so called inverted mass hierarchy and the presence of sterile neutrinos - simply emphasise the lack of clear theoretical guidance and justify the many searches for neutrino oscillation in different regions of the parameter space (Δm^2, $sin^2 2\theta$).

Current experiments, such as CHORUS and NOMAD [7, 8], will shed light on $\nu_\mu \rightarrow \nu_\tau$ mixing for large mass differences. SOUDAN 2 [9] and SUPERKAMIOKANDE [10] presumably will establish with certainty the atmospheric neutrino anomaly. In this context, it is worth noting that a recent analysis, by the Superkamiokande collaboration, of the azimuthal dependence of the combined ν_μ and $\bar{\nu}_\mu$ fluxes, has updated the preferred value for $\Delta m^2_{\mu\tau}$ from $\sim 10^{-2} eV^2$ to $\sim 10^{-3} eV^2$, demonstrating therefore that the experimental scenario is far from settled [11].

CHOOZ [12], studying the possible disappearance of $\bar{\nu}_e$ at energies of a few MeV, is in a position to rule out or confirm $\nu_\mu \rightarrow \nu_e$ transitions as an explanation of the effect observed in the atmospheric neutrino flux.

KARMEN [13], after the recent upgrade with the addition of an active veto shield, should be able to confirm the findings of LSND, although in the region $\Delta m^2 \sim 0.1 - 1\, eV^2$, of particular interest from the cosmological point of view, it barely covers the 90% likelihood contour of LSND.

In spite of the fact that new - and potentially decisive - results are forthcoming, another generation of experiments are already in preparation in Europe, USA and Japan to explore and extend the searches to a larger area of parameter space.

BOREXINO [14] will establish whether indeed the solar neutrino flux is reduced in an energy dependent fashion, and SNO [15] will count neutrinos of all flavours, thus choosing between the solar model or particle physics origin of the reduction.

Accelerator based experiments, using neutrino sources located at distances of several hundreds of kilometers from the detectors (K2K [16], MINOS [18], CERN beam to Gran Sasso [17]), would check whether the effect seen in the atmosphere is observable also with beams which can be controlled and whose composition is better known.

Furthermore, experiments like COSMOS [19] and TOSCA [20] (called short baseline, because the detector typically is at less than 1 km from the source) have been proposed to extend the search for $\nu_\mu \rightarrow \nu_\tau$ oscillation to regions of mixing angle smaller than 10^{-4}.

In the $\nu_\mu \rightarrow \nu_e$ channel, BooNE [21], an experiment that would develop in two phases, is the only proposal whose aim is to probe smaller (than LSND) mixing angles in the $0.1 - 1\,\mathrm{eV}^2$ mass region. Experiments addressing the same issue were proposed at CERN [22, 23] but were superseded by plans for long baseline experiments.

We believe that the parameter region ($\Delta m^2 \sim 1\,\mathrm{eV}^2, sin^2 2\theta \sim 10^{-3}$), as mentioned earlier, is interesting and worth exploring in its own right, regardless of the LSND claim, given that neutrinos with a mass of order of 1 eV have an important role in cosmology and are possible candidates for hot dark matter [24]. Therefore a new experiment capable of reaching such limits should be performed. At the same time, this would allow a thorough check of the LSND experimental result. The findings of such a new experiment would be more significant if it were performed at L/E comparable to that of LSND but in a completely different energy regime and if the technique employed and the systematics were different from LSND.

To this purpose the low energy ($\langle E_\nu \rangle \sim 1.5\,\mathrm{GeV}$) neutrino beam from the CERN-PS could prove very valuable. Therefore, in this document, its use is envisaged for a high sensitivity $\nu_\mu \rightarrow \nu_e$ oscillation experiment, on a time scale that allows physics results to be obtained in the year 2002, thus exploiting at its best the potential of CERN. This can be achieved since, with standard techniques and very few developments required, a detector may be constructed in a relatively short time thus allowing data taking in the years 2000-2001.

Should the search be successful, then improvements are feasible [25] that aim at a reduction of the ν_e contamination in the beam making possible a precise measurement of Δm^2.

This document is organised as follows. The principle and capabilities of the experiment are summarised in section 2, while the following sections give more detailed information. The beam line and expected performances are given in section 3 and the detector is described in section 4. The event selection, signal and backgrounds are thoroughly discussed in section 5 and the sensitivity to the oscillation parameters is analysed in section 6.

2 The Experiment

2.1 Principle and capabilities of the experiment

The primary objective of this experiment is to search for the appearance of electron neutrinos in a ν_μ beam of about 1.5 GeV average energy through a comparison of ν_e charged current interactions in detectors located at two different distances (130 and 885 meters) from the proton target. This is possible by restoring the neutrino line from the CERN-PS and using existing experimental halls. Unlike the case of disappearance experiments, the detector located at the closer site is **not** used to predict the ν_μ flux, but rather to measure the relative ν_e/ν_μ interaction rate. With the estimated ν_e and $\bar{\nu}_e$ contamination in the proposed beam, and in the absence of any other phenomenon, this relative rate is about 6×10^{-3}. If $\nu_\mu \rightarrow \nu_e$ oscillations take place, then at the far location, another detector - identical in structure to the detector at the close site - would measure a larger ν_e/ν_μ ratio. The experimental layout is shown in figure 2.

At the far site, the detector consists of two identical modules to exploit the space available in the existing experimental hall. This configuration also helps in the assessment of the systematic errors arising from the angular dependence of the ν_e contamination. The aim of the experiment described in this document, is to measure the ratio ν_e/ν_μ (as a function of energy and integrated over all energies) with high statistical significance for oscillation probabilities down to 10^{-3} for $\Delta m^2_{e\mu} \sim 1$ eV^2.

All three detector modules have the same simple structure, made of a fine grained *tracking calorimeter* that constitutes the neutrino target, followed by a *tail catcher* and a *muon catcher*. The fully active tracking calorimeter is made out of a succession of 300 layers of plastic scintillator and streamer tube planes, for a total mass of 128 t. The detector at the 885 m site, made out of two modules, will have a total mass of 256 t. In the calorimeter, particle trajectories and energy loss are both sampled every 0.1 X_0.

The tail catcher and the muon catcher have the same structure as the tracking calorimeter, with coarser granularity obtained with the addition of a suitable passive absorber. The dominant factor in the choice of detector type is the relatively short time scale foreseen for the experiment that does not allow for extensive detector R & D.

The neutrino reactions that will be selected are the quasi-elastic channels:

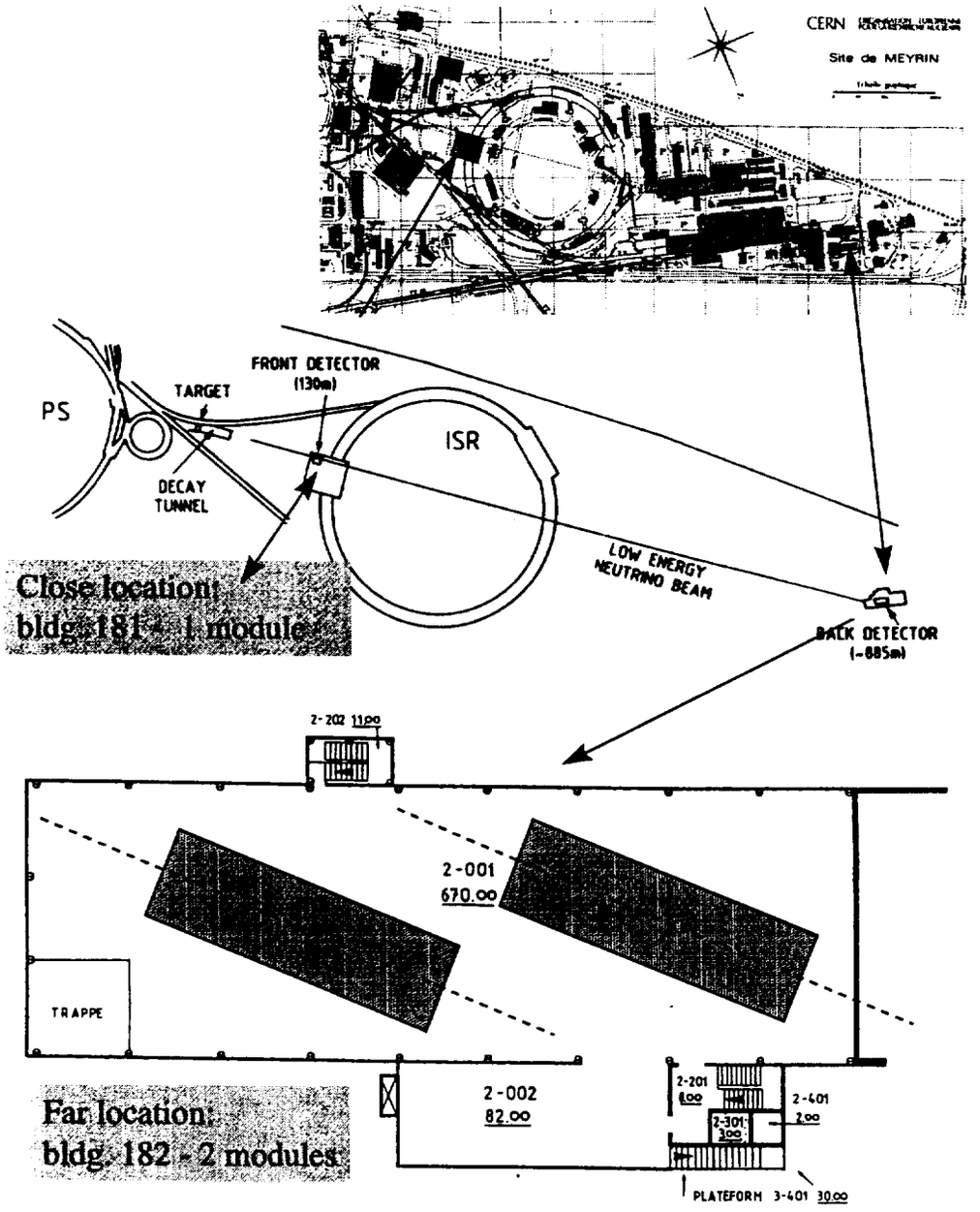

Figure 2: Layout of the experiment

$$\nu_e \, n \rightarrow e^- p \qquad (1)$$

$$\nu_\mu \, n \rightarrow \mu^- p \qquad (2)$$

which, at the energies involved, account for about 50% of all charged current interactions. It should be observed that, near the neutrino interaction vertex, these reactions have an identical signature: a minimum ionizing particle accompanied by a heavily ionizing proton, whose signal is often detected in the scintillator and, less frequently, by the tracking elements. Further downstream from the vertex, reaction (1) is characterized by the presence of an electromagnetic shower initiated by the electron, while the signature of reaction (2) is a penetrating minimum ionizing particle.

At the two locations, the ratio N_e/N_μ, of the number of events assigned to reactions (1) and (2) respectively, will be measured. In particular, the quantity

$$\Delta = \left(\frac{N_e}{N_\mu}\right)^{FAR} - \left(\frac{N_e}{N_\mu}\right)^{CLOSE}$$

will be determined, and the error on the determination of Δ will be the limiting factor in the sensitivity to neutrino oscillation.

In the absence of oscillations N_e, the number of events experimentally assigned to reaction (1), receives contributions from genuine ν_e ($\bar{\nu}_e$) quasi elastic interactions and from neutral current interactions where electromagnetic activity (from π°decay) simulates the quasi elastic pattern.

Similarly N_μ, the number of events experimentally assigned to reaction (2), receives contributions from genuine ν_μ and $\bar{\nu}_\mu$ quasi elastic interactions, and neutral current events in which a charged pion is mistakenly identified as a muon. It should be observed that N_μ is used as a normalisation and therefore what is important is not which specific channel is selected but rather that the close and far detectors select the same channels.

The expected event rates and the sensitivity of the experiment will be evaluated assuming $2.5 \cdot 10^{20}$ protons on target, an intensity which could be collected in a two years run (see section 3). The corresponding numbers of genuine quasi-elastic ν_μ interactions in the close (128 t) detector and far (256 t) detector are $2.86 \cdot 10^6$ and $1.3 \cdot 10^5$, respectively.

Selection criteria and evaluation of efficiencies, described in section 5.2, allow to compute the observed numbers of events N_μ and N_e. They are listed in Table 1, where the corresponding values for Δ are also given.

Table 1: Number of electron and muon quasi-elastic events observed by this experiment under different hypotheses. The resulting values for Δ (defined in the text) are given for the case of no oscillation and for $\Delta m^2_{e\mu} = 2\,eV^2$ and $sin^2 2\theta_{e\mu} = 0.006$.

	Close	Far	Δ
N_μ	1.87×10^6	0.85×10^5	
N_e $(P = 0)$	6813	309	$(0.0 \pm 0.2)10^{-3}$
N_e $(2\,eV^2, 0.006)$	7480	604	$(3.10 \pm 0.29 \pm 0.10) \times 10^{-3}$

In the absence of oscillations, Δ should be equal to zero within errors. In fact, since the close and far detectors are identical, any contamination is properly accounted for by taking the difference of the ratios, and thus a precise evaluation of each individual contribution is not required, although, to increase the sensitivity to oscillations, it is desirable that the total background be small. A non-zero value of Δ (beyond statistical fluctuations)[1] would be a clear indication for neutrino oscillation.

In table 1 we give an example of the results which would be obtained for $\Delta m^2_{e\mu} = 2\,eV^2$ (where our sensitivity is maximal) and $sin^2 2\theta_{e\mu} = 0.006$ (the corresponding mixing angle of the LSND claim). In this case the experiment would observe an excess of 295 events in the far detector, measuring $\Delta = 3.10 \pm 0.29 \pm 0.10$, which is different from zero by more than 10 standard deviations.

Should the measured value of Δ be consistent with zero, then the experiment would obtain the curve shown in figure 13 as 90% C.L. limits on the oscillation probability.

As figure 13 shows, the sensitivity in the region $\Delta m^2 \sim 1 eV^2$, is much larger than that of previous experiments performed with a similar beam, at the Brookhaven AGS and at the CERN PS. This is due to the combination of three items: high statistics (intense use of the PS beam and large detector mass), good electron identification, and two detectors technique (close and far) for a safe control of the backgrounds.

The use of two detectors is the main reason for improvement, when compared with experiments of similar statistics performed at the AGS of Brookhaven (BNL 776 [26], BNL 734 [27]). In fact, aiming at detecting os-

[1] Δ could be negative in the scenario in which oscillations occur already at the location of the close detector.

cillation probabilities of the order of 10^{-3} or less, one has to reach a very good control of the background. For instance, single π° events which could fake electron events, have to be reliably suppressed by a factor 500 or more. Only if the residual contamination is measured in a close detector, can the related systematic error be neglected.

Searches for neutrino oscillation using the PS beam have been performed by the CDHS [33] and CHARM [32] collaborations, with the close/far detector technique. The statistics was however much lower and, due to the limited capability of identifying electrons, the main results were obtained in the ν_μ disappearance search. Interesting limits on $\nu_\mu \rightarrow \nu_e$ oscillations were obtained by the BEBC experiment [29], exploiting the unmatched pattern recognition power of bubble chambers. The total statistics was however of the order of 500 ν_μ interactions only.

In the future, the main competitor to the experiment proposed here could be the BooNE experiment, already mentioned above, now being proposed at Fermilab. The detection technique would be similar to that used by LSND and the neutrino energy will be in the range 0.15 to 1 GeV. If approved, in a first phase, the MiniBooNE experiment plans to reach a sensitivity similar to ours, with a single 400 t detector at 1000 m from the neutrino source. Final results would be available in year 2003. A second phase, with the construction of a close detector for a better control of the backgrounds, is only foreseen in case MiniBooNE finds evidence for oscillation [21].

3 The neutrino beam

3.1 The PS neutrino beam line

The requirements imposed on the neutrino beam can be summarized as follows:

- the muon neutrino flux at the far detector must be as large as possible;
- the energy spectrum must be peaked at around 1 GeV, to match the Δm^2 region we are proposing to investigate, and rapidly falling above 2.5 GeV, to reduce π° background;
- the contamination of electron neutrinos should be kept at the lowest possible level.

As a starting point we have considered the beam set-up used by the BEBC-PS180 [29] $\nu_\mu \rightarrow \nu_e$ experiment. In that experiment the 19.2 GeV/c proton beam was extracted from the PS and impinged on a 80 cm long, 6 mm diameter beryllium target. This was followed by a magnetic horn designed to optimally focus positive particles of momentum around 2 GeV/c. After focusing the particles propagated in a decay tunnel of about 50 m length and of $3.5 \times 2.8\,m^2$ cross section for the first 25 m and of $5.0 \times 2.8\,m^2$ for the remaining 25 m to allow the decay of mesons with a larger angular divergence with respect to the beam axis. The decay tunnel was then followed by iron shielding of 4 m thickness and by about 65 m of earth where all remaining hadrons and most of the muons were absorbed. The open symbols of figure 3 show the resulting neutrino spectra at the BEBC location (825 m) as predicted by their simulation. The mean energy of the ν_μ is about 1.5 GeV, while the 0.4% ν_e component has a mean energy of about 2.5 GeV.

Some beam elements of the old PS TT7 line are still existing and working and can be re-used by the proposed experiment. Moreover the close detector station could be placed in the existing pit, at a distance of about 130 m from the target, that was used by previous oscillation experiments [31],[32],[33], while the far detector can be located in the CharmII [34] experiment hall at about 885 m distance from the target.

3.2 Beam simulation

To study the relevant features of the neutrino beam at the two detector locations a GEANT based simulation program has been developed. It includes the elements of the BEBC beam set-up described in the previous section. The hadronic interactions in the beryllium target are generated by the FLUKA generator available in GEANT [35].

In figure 3 the spectra predicted by this simulation for ν_μ and ν_e neutrinos at 885 m from the target are shown. As a comparison the results of the BEBC simulation are superimposed, showing that the main features of the spectra are reproduced in a similar way by the two Monte Carlo. An optimization study and a finer tuning of the input parameters should however be done. Several measurements of hadron production exist at these proton energies [36] which can be used to cross check the outcome of the FLUKA generator and improve the reliability of the simulation.

As described earlier, relevant to our experiment is the contamination of $\nu_e(\bar{\nu}_e)$ and its variation along the path to the two detection positions. In figure

4 the flux ratio $(\nu_e + \bar{\nu}_e)/(\nu_\mu + \bar{\nu}_\mu)$, integrated over ν energies, is shown as a function of the distance from the target. The average contamination is of the order of 0.6% with no energy cut and about 0.3% imposing a cut on the electron neutrino energy similar to that required in the reconstruction (section 5). The relative difference at the two detector locations is of the order of $\pm 7\%$. Even with the pessimistic assumption of a 50% uncertainty on this difference, the final sensitivity to oscillations is still dominated by the statistical uncertainty, as discussed in section 6. The energy distributions of the two main neutrino components do not show significant differences at the two locations as can be seen in figure 5.

3.3 Requirements on proton intensity

The total number of protons on target (PoT) needed to provide the integral neutrino flux for the proposed measurement is about $2.5 \cdot 10^{20}$. We assume the same beam parameters as in the BEBC experiment. From discussions with the machine experts [37], the CERN proton acceleration complex appears, in principle, capable of providing this number of protons in about two years of operation.

Protons originate in the proton linac (LINAC II) and are accelerated first in the Booster (PSB) and then in the PS machine. This operates in a supercycle which is a multiple of the repetition time of the booster, 1.2 s. In figure 6 the 14.4 s supercycle currently in use is shown. It consists of 12 PSB 1.2 s cycles.

The maximum number of protons that can be accelerated in each PS cycle is limited by the booster to $3.0 \cdot 10^{13}$. A much more stringent limit to the total amount of protons that the PS can deliver to users comes, however, from machine losses. These should be kept below $5 \cdot 10^{11}$ p/s. As they presently amount to about $5 - 10\%$ of the accelerated beam, the average intensity of protons circulating in the PS is limited to 5 to $10 \cdot 10^{12}$ p/s. Among the upgrades necessary for operation of the LHC is the injection of protons from the PSB to the PS at an energy of 1.4 GeV instead of 1 GeV, leading to a reduction of beam losses due to the lower emittance. It appears therefore reasonable to assume that it will be possible to accelerate $10 \cdot 10^{12}$ p/s in the PS.

According to 1996 performance one year of PS operation corresponds to about 6800 hours at about 92% efficiency. At the average intensity above, $2.3 \cdot 10^{20}$ PoT per year could be delivered to users. At the moment we do not

know of any other request for high proton intensities in the years 2000-2001 when we propose to take data. The WA neutrino beam should no longer be in operation and the proposed Gran Sasso neutrino beam may not have begun yet. The SPS will only need to run at limited intensities. It is therefore conceivable for our proposed experiment to collect a large fraction of the total protons from the PS and complete its data taking within about two years.

Assuming for instance the present supercycle duration and the 1996 PS performance an intensity of about $7.5 \cdot 10^{13}$ PoT/14.4 s, i.e. $5 \cdot 10^{12}$ p/s, would fulfill our requirements. One way to accomplish this is to use three out of the total twelve 1.2 s cycles in the present 14.4 s supercycle (fig. 6). During each cycle $2.5 \cdot 10^{13}$ PoT could be accelerated and extracted towards the neutrino target. Some PS cycles will become available with the closing of LEP while others will be required by new users. After discussion with PS division experts, although a precise scheme has not been worked out, there seems to be more than one scenario capable of accommodating the necessary proton intensity, while respecting the limitations imposed by the operation of the acceleration complex.

4 The Detector

An important aspect of the proposed experiment is the capability to be ready for data taking in the year 2000. For this reason the detector should rely on standard techniques. Here we consider a very simple structure which has been used to measure rates and efficiencies in our simulation program. A study of an improved design, with optimisation of the choice of the active elements, of the detector mass and granularity, and of the readout system, is in progress.

We have considered three identical modules; one module for the close detector, and two modules constituting the far detector (see figure 2).

A detector module consists of a fine-grained *tracking calorimeter*, followed by two sections with coarser sampling: the *tail catcher*, to fully contain and measure the electromagnetic showers, and the *muon catcher*, to extend the muon identification and momentum measurement.

One tracking calorimeter consists of 300 planes of streamer tube chambers, alternated with 300 scintillator planes. The streamer tube chambers and the scintillators act as the target for neutrino interactions.

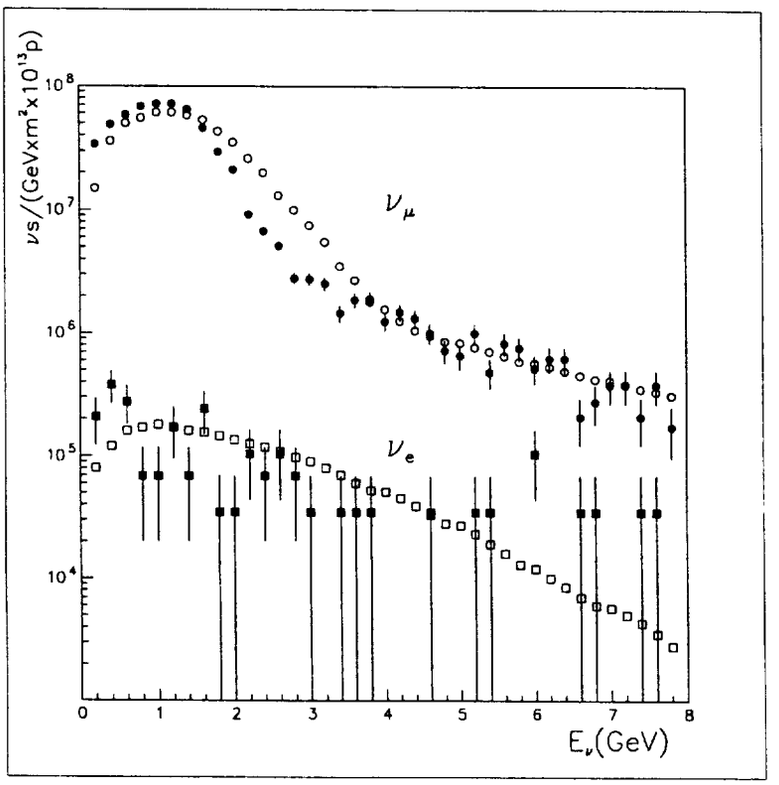

Figure 3: ν_μ (circles) and ν_e (squares) spectra: BEBC simulation (open symbols), this simulation (full symbols).

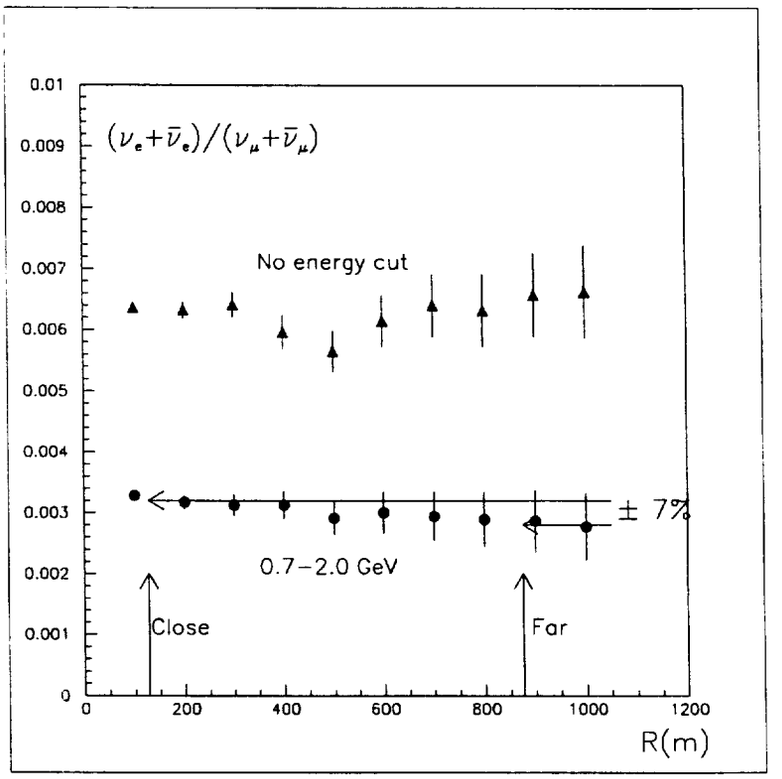

Figure 4: Relative integral fluxes of total electron neutrino component as a function of the distance from the target. The data points at different distances are correlated and the errors are statistical only.

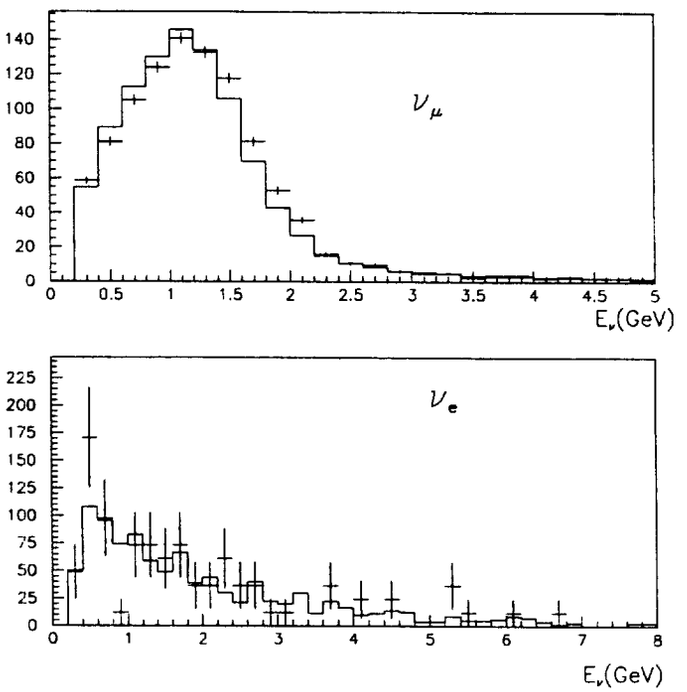

Figure 5: Spectra of ν_μ (top) and ν_e (bottom) at $R = 130\,\mathrm{m}$ (full line) and at $R = 885\,\mathrm{m}$ (points with error bars).

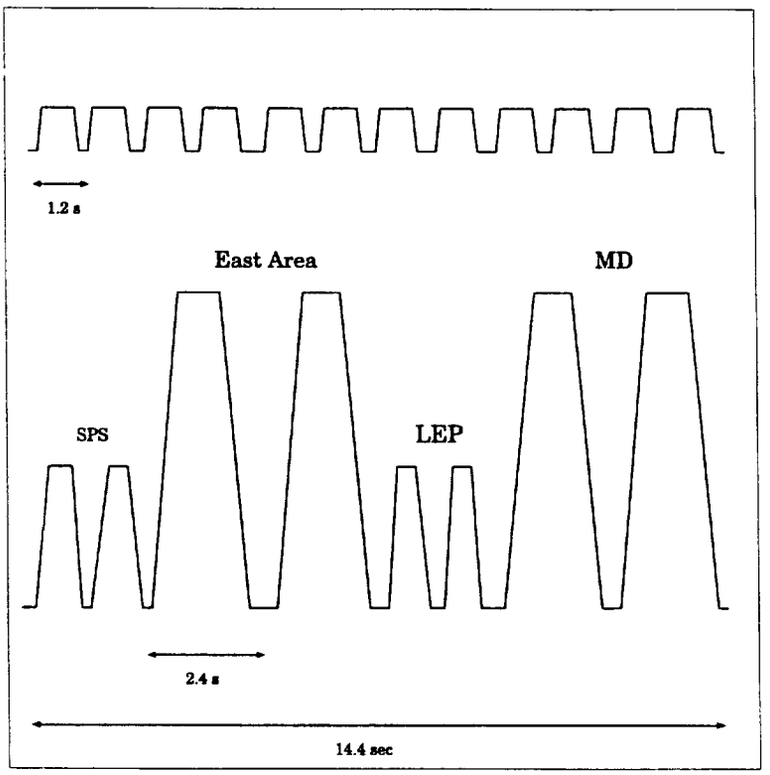

Figure 6: PS supercycle structure.

The 420 streamer tube chambers used by the CHARMII experiment [34] are still in good conditions (some of them have been installed in the CHORUS detector), and could be re-employed, if the CHARMII collaboration agrees. Each chamber consists of 352 square-shaped limited streamer tubes with an inner area of $9 \times 9\,\mathrm{mm}^2$, an average wire spacing of 1.05 cm, and a length of 367 cm, for a total active area of $367 \times 367\,\mathrm{cm}^2$ per plane. A digital readout of the wire signal is foreseen, as in CHARMII, where an efficiency close to 100% was measured for large angle tracks (for straight tracks, due to the tube walls, the efficiency is $\sim 90\%$).

Each streamer tube chamber is followed by a plane of scintillators, consisting of 15 individual strips of 24.5 cm width and 2 cm thickness, each oriented parallel to the wires of the preceding streamer tubes plane. The choice of the read out system is in progress, and at this stage is not essential. We are aware that there exist readout systems alternative to photomultipliers, that would allow a significant reduction in the actual number of photon detectors to handle, such as the coupling of the scintillator strips, through wave length shifting fibres, to multianode photomultipliers [38].

For the full calorimeter a modular structure consisting of 75 basic units (fig. 7) has been considered. Figure 8 shows a basic unit, made of 4 streamer chambers and 4 scintillator planes, with alternating horizontal and vertical orientations, to be assembled in a structure of 20 cm thickness. The streamer tubes of the four chambers of a basic unit are staggered half a tube with respect to each other to optimise the geometrical acceptance. Each streamer tubes chamber corresponds on average to 0.043 radiation lengths; each scintillator plane to 0.047 radiation lengths.

The tracking calorimeter has a front surface of $3.67 \times 3.67\,\mathrm{m}^2$ and a length of 15 m (27 radiation lengths and 10 interaction lengths). The average density is about $0.63\,\mathrm{g/cm}^3$, for a total mass of 128 t.

At the end of the tracking calorimeter a tail catcher of about 12 radiation lengths provides the longitudinal containment of electromagnetic showers and the energy measurement for interactions produced in the last part of the tracking calorimeter. The tail catcher consists of 20 scintillator planes, interleaved with 1 cm thick iron absorbers. It is followed by a muon catcher consisting of a sandwich of 10 planes of streamer tubes and of 10 cm thick iron absorbers.

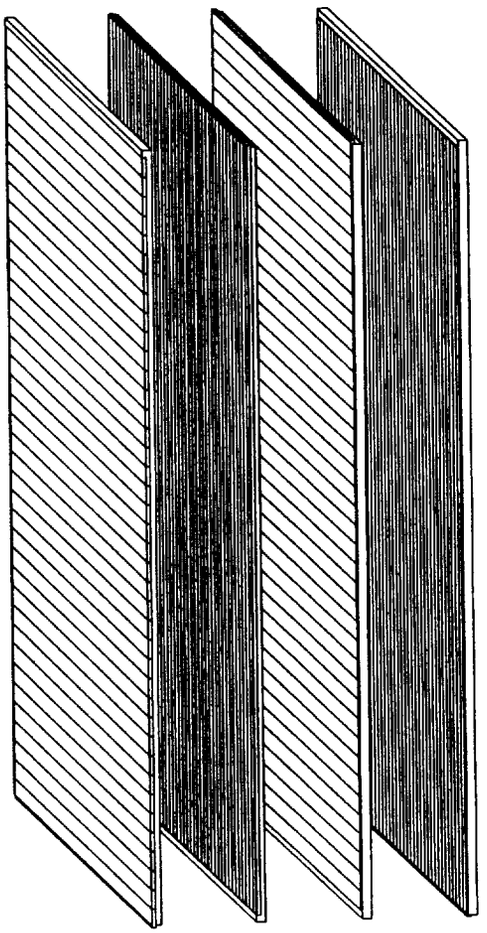

Figure 7: Expanded structure of a basic unit.

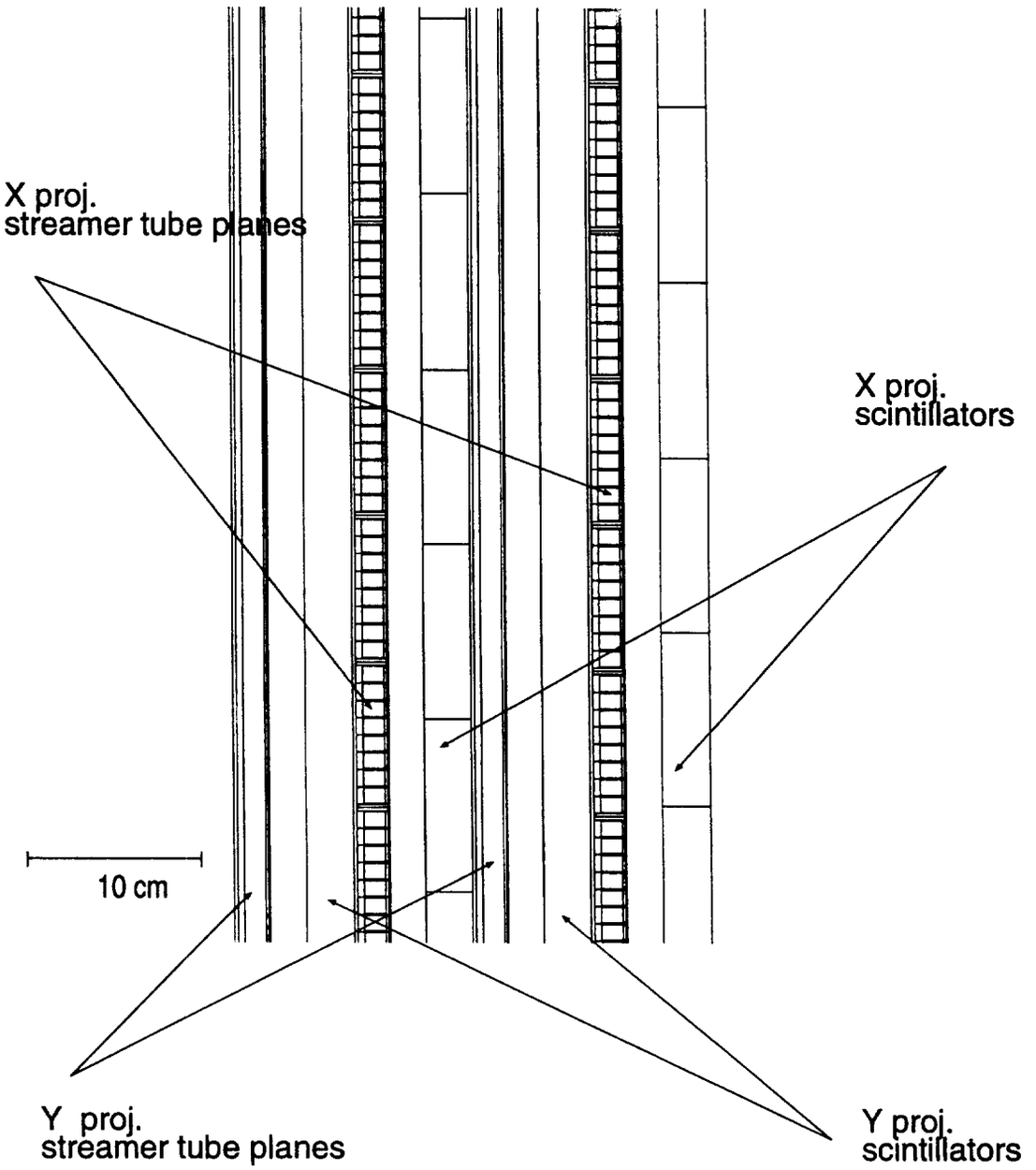

Figure 8: Details of a basic unit.

5 Signal and background

5.1 Low energy neutrino interactions

To evaluate the sensitivity to the signal and the contributions to the background, we have simulated events with a generator which phenomenologically includes the experimental results on low energy neutrino interactions available in the literature. In the event generation, we have taken into account the quasi-elastic reaction, and, both for NC and CC reactions, the production of resonances and the onset of the deep inelastic processes. The generator also includes the energy dependence of the different cross sections. The absolute normalisation, used in computing event rates, has been based on a cross section $\sigma = 0.85 \times 10^{-38}\,\mathrm{cm}^2$ for the quasi-elastic scattering $\nu_\mu \mathrm{n} \rightarrow \mu^- \mathrm{p}$, measured in a comparable energy range [27].

Events have been generated according to the energy distribution of neutrinos from the PS neutrino beam. Results concerning the fractions of events in each final state are presented in table 2 and 3 for CC and NC reactions respectively. They agree with those produced by a similar generator used by the CHORUS collaboration [28].

The results of the generator have been compared with existing measurements. As an example, table 4 shows the rates predicted by the generator for various CC reactions, compared with those measured in the PS beam by BEBC [29].

Another check concerns the ratio of neutral to charged current production of single π° events. This check is important because π° production in neutral current events constitutes the main background to ν_e quasi-elastic interactions. The Aachen-Padova collaboration [30] quotes for the ratio

$$R_0 = \frac{\sigma(\nu_\mu + N \rightarrow \nu_\mu + \pi^\circ + N')}{\sigma(\nu_\mu + N \rightarrow \mu^- + \pi^\circ + N')}$$

the value $R_0 = 0.94 \pm 0.12$ in agreement with our result of $R_0 = 1.06 \pm 0.10$ (our value of R_0 was calculated reproducing the experimental cuts of the Aachen-Padova analysis and therefore cannot be directly obtained from the numbers in the tables).

In conclusion we are confident that our generator gives a reasonable description of low energy neutrino interactions. We stress however, that in the experiment the background subtraction will be based on measurements at

the close detector and will not rely on Monte Carlo descriptions of quantities like R_0.

final state	rate(%)
μ p	40.5
$\mu\,\pi^+$ p	15.5
$\mu\,\pi^\circ$ p	7.8
$\mu\,\pi^+$ n	7.1
$\mu\,\pi^+\,\pi^-$ p	2.8
$\mu\,\pi^\pm\,\pi^\circ\,N$	5.3
$\mu\,3\pi\,N$	-
total CC	79.

Table 2: Relative rates of different charged current interactions.

final state	rate(%)
$\nu\,\pi^+$ n	3.0
$\nu\,\pi^\circ$ p	3.0
$\nu\,\pi^\circ$ n	3.0
$\nu\,\pi^-$ p	3.0
$\nu\,\pi^+\,\pi^\circ$ n	2.2
$\nu\,\pi^+\,\pi^-\,N$	1.1
$\nu\,\pi^-\,\pi^\circ$ p	1.1
ν p	4.4
total NC	21.

Table 3: Relative rates of different neutral current interactions.

5.2 Event simulation and selection

We recall that the oscillation signal is represented by an excess of quasi-elastic $\nu_e n \rightarrow e^- p$ interactions, with respect to the few events due to the ν_e

final state	BEBC(%)	our generator(%)
quasi elastic	61	51
single pion prod	32	39
>1 pion production	7	10

Table 4: Relative rates of charged current events: comparison with BEBC data [29].

and $\bar{\nu}_e$ components of the beam. The choice of this channel is motivated by the fact that at low energy it constitutes a large fraction ($\sim$ 50%) of the total CC cross section. Moreover, quasi-elastic events can be clearly identified in the detector and have little background from ν_μ induced reactions.

The number of events experimentally classified as $\nu_e n \rightarrow e^- p$ interactions has contributions from the following sources:

- genuine ν_e ($\bar{\nu}_e$) quasi elastic interactions, either from contamination in the beam or from $\nu_\mu \rightarrow \nu_e$ ($\bar{\nu}_\mu \rightarrow \bar{\nu}_e$) oscillations;
- inelastic charged current interactions initiated by ν_e in which some charged particles are missed.
- $\nu_\mu e \rightarrow \nu_\mu e$ elastic scattering;
- neutral current interactions (initiated by ν_μ or by ν_e) where electromagnetic activity (from π° decay) simulates the quasi elastic pattern.

The main contribution to the background is expected to come from ν_μ NC interactions with a π° in the final state. The number of events expected from elastic scattering of ν_μ on electrons is one order of magnitude smaller than that due to the ν_e and $\bar{\nu}_e$ components of the beam and will therefore be neglected in the following.

The generator discussed in the previous section has been used to simulate neutrino interactions in the detector described in section 4. The detector response has been fully simulated with GEANT. Figures 9 and 10 show two examples of the detector response to different neutrino interactions.

The selection of the quasi-elastic $\nu_e n \rightarrow e^- p$ reaction is based on the following criteria: the event pattern is a clear electromagnetic shower initiated by a single charged track, the electron, and accompanied at most by a second charged track (visible or invisible proton).

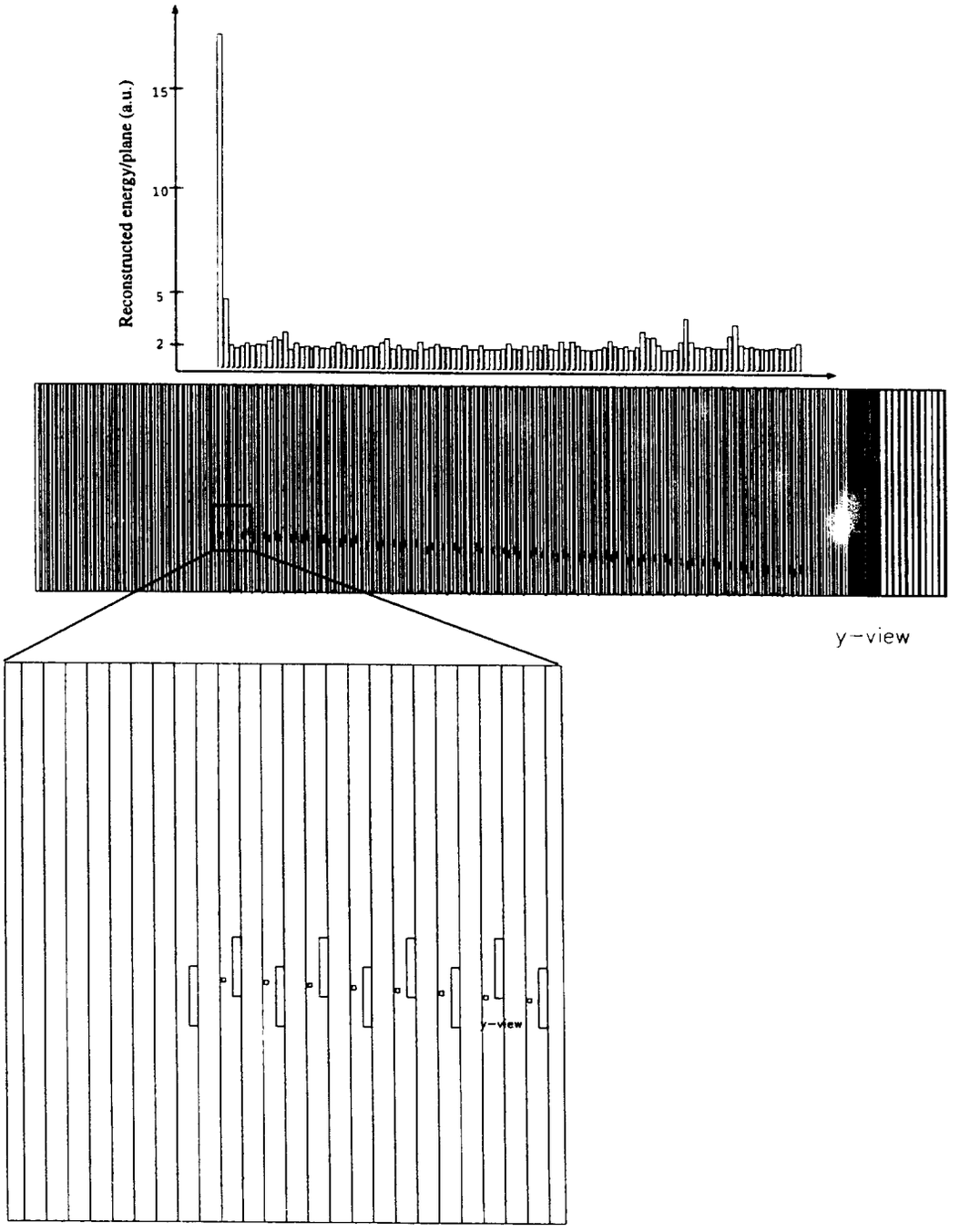

Figure 9: A ν_μ quasi elastic interaction. The energy loss of the proton in the first two scintillator planes is visible.

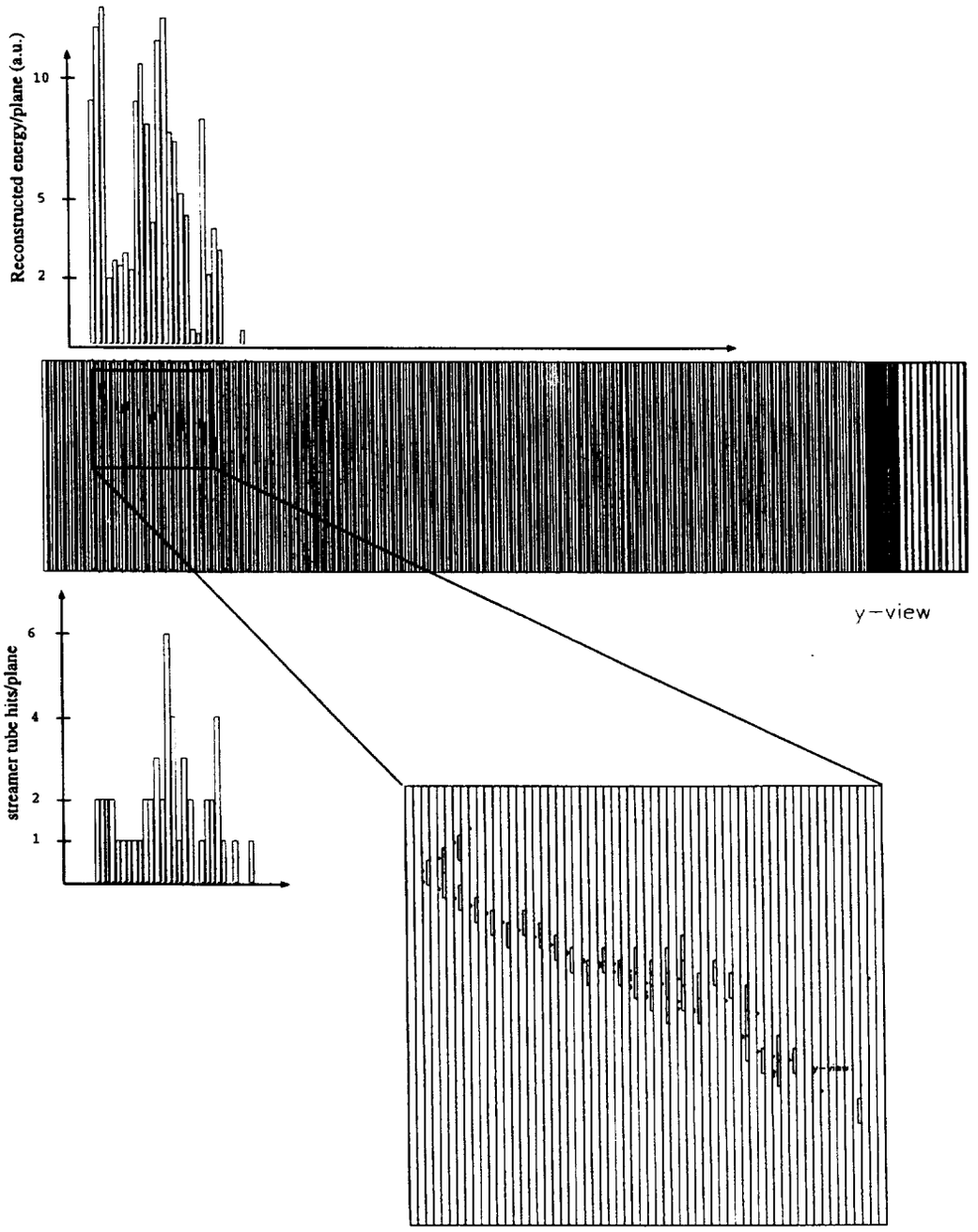

Figure 10: A ν_e quasi elastic interaction. The electron shower is connected to the vertex by a minimum ionizing particle.

As can be seen in figure 10, electron induced electromagnetic showers show a well characterised pattern, with clusters of hits in the streamer tubes, associated with a large activity in the scintillators. The energy resolution for isolated electrons is 5.5 % at 1 GeV for showers contained in the tracking calorimeter. The resolution is slightly worse for showers leaking in the tail catcher.

The rejection of ν_μ interactions with π° production is obtained with the two criteria discussed hereafter: a cut on the electromagnetic energy of the event and a selection based on the difference in pattern between electromagnetic showers initiated by electrons and π°'s .

Figure 11 shows the distribution of the energy of π°'s produced in ν_μ NC interactions, together with the energy distributions of the electron from $\nu_e n \rightarrow e^- p$ scattering for events from oscillation. The electron energy distribution has beeen computed assuming that the ν_e energy spectrum has the same form as the ν_μ spectrum. The ν_e rate corresponds to the mixing $sin^2 2\theta_{e\mu} = 6 \times 10^{-3}$. It is seen that the π° background can be strongly reduced by requiring a minimum energy.

Further background reduction can be obtained by exploiting the high granularity of the detector, which allows a good separation based on the activity at the beginning of the shower. As an illustration, figure 12 shows the different behaviour of signals from electrons, π°'s and muons in the first and fifth scintillator planes following that where the neutrino interaction took place. Because of the high sampling frequency, the electron often behaves like a minimum ionising particle, depositing an amount of energy similar to that of the muon and half of that of a converted gamma.

Combining the effect of the energy cut and of the difference in shower pattern, the background from π° production can be suppressed to a level below the unavoidable ν_e and $\bar{\nu}_e$ contamination.

A preliminary analysis of the simulated data was performed to compute the efficiency for the signal and the power of background rejection. This was based on a visual blind scan of events by several operators.

The cut applied on the electromagnetic energy of the event was $E_e > 0.8\,\mathrm{GeV}$ (to reduce the π° background) and $E_e < 2.2\,\mathrm{GeV}$. The high energy cut was used to eliminate part of the background due to the ν_e and $\bar{\nu}_e$ components of the beam which have a harder spectrum than the ν_μ component, and hence a harder spectrum than the ν_e events from oscillations.

For the signal, the quasi-elastic interactions of ν_e from oscillations, the efficiency of the energy cut is 60%. The sample is further reduced by 0.80,

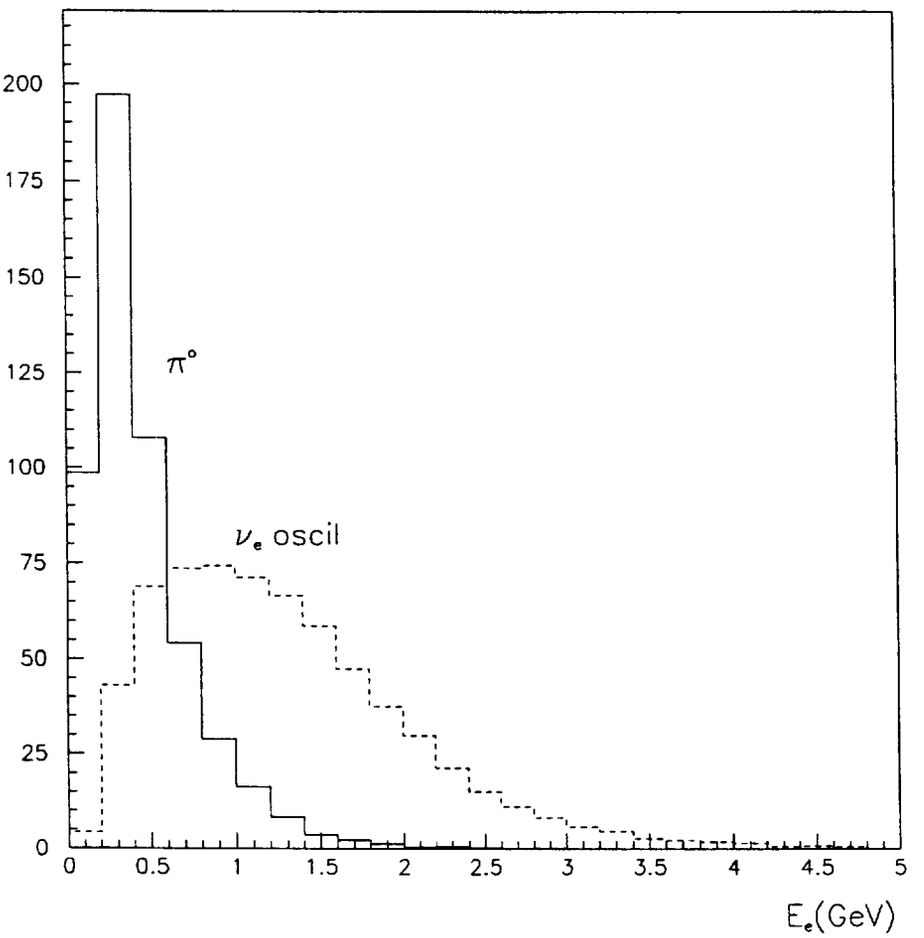

Figure 11: Energy spectra of electrons (ν_e from oscillation.) and π°'s (from ν_μ NC interactions)

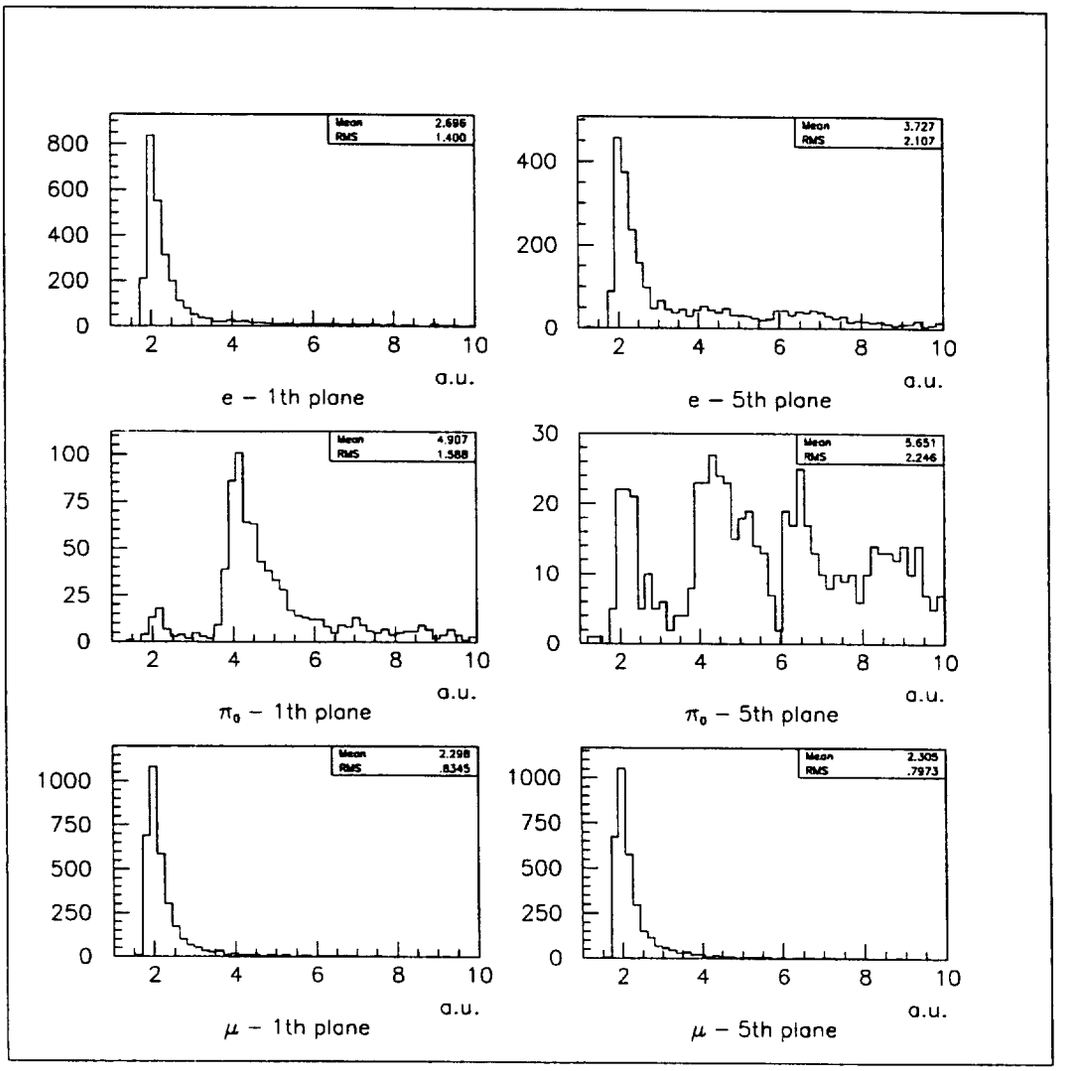

Figure 12: Energy deposited by electrons, π° and muons in the first and fifth scintillator plane following the neutrino interaction vertex.

	$\nu_e + \bar{\nu}_e$ contamination (q.e.)	ν_μNC with π°
ϵ_0 (= rate without cuts)	0.006	0.2
ϵ_1 (energy cut)	0.40	0.12
ϵ_2 (pattern in detector)	0.8	0.02
$\epsilon_0 \times \epsilon_1 \times \epsilon_2$	0.0019	0.0005

Table 5: Rates and efficiency of selections for background events.

when requiring the pattern of quasi-elastic interactions. The overall efficiency is then $\epsilon = 0.6 \times 0.8 = 0.48$. Note that the efficiency depends on the energy spectrum of the oscillated neutrinos. The quoted numbers were computed assuming for the ν_e the energy spectrum of the ν_μ beam.

The results for the background are summarised in Table 5, separately for the quasi-elastic interactions of the ν_e contaminating the beam, and for the NC interactions of ν_μ with π° production. In the first line, for both backgrounds, we give the expected rate, relative to the number of quasi elastic ν_μ interactions. The product of the expected rate times the efficiencies is given in the last line. The numbers turn out to be small, especially when compared with the efficiency for the signal.

6 Sensitivity to Oscillation

As was discussed in section 2, the variable that will be used to detect possible oscillations is

$$\Delta = \left(\frac{N_e}{N_\mu}\right)^{FAR} - \left(\frac{N_e}{N_\mu}\right)^{CLOSE} = R^{FAR} - R^{CLOSE}$$

with

$$N_e = N^{osc} + N^{\nu_e} + N^{\pi^\circ}$$

where we have explicitly indicated the various sources that contribute to the observed number of events (N^{π° being the number of events in which a π° is wrongly identified as an electron). As far as N_μ is concerned, it is worth recalling that the effect of the contamination of charged pions in the muon

sample is negligible, provided that the close and far detectors measure it in the same manner.

With 2.5×10^{20} PoT in two years of data taking and 256 t mass for the far detector, we expect about 130 thousand interactions of the type $\nu_\mu n \rightarrow \mu^- p$ of which 85000 will be identified as such. The number of identified electron neutrino quasi elastic interactions, from the 0.6% contamination in the beam, given the efficiency in table 5, will be $N^{\nu_e} = 248$. N^{π° has been estimated to be 61.

For $\Delta m^2 = 2\,eV^2$ and $sin^2 2\theta = 6 \times 10^{-3}$ (approximately the central value of the mixing angle of LSND for this Δm^2), the close and far detectors would measure $R^{CLOSE} = (4.00 \pm 0.05(stat)) \times 10^{-3}$ and $R^{FAR} = (7.10 \pm 0.29(stat)) \times 10^{-3}$ respectively. The difference turns out to be

$$\Delta = (3.1 \pm 0.29(stat) \pm 0.10(syst)) \times 10^{-3}$$

where the systematic error, arising from the difference in the ν_e contamination at the two sites, was assumed to be 3.5% (see section 3.2). The use of two identical detectors allows other sources of systematic errors to be neglected. With the above values of the parameters, the oscillation signal is established with a significance of 10 standard deviations.

In the absence of oscillation, the upper limit on Δ may be used to draw the contour of an excluded region in the parameter space and this is shown in figure 13.

Further improvements of the sensitivity can be obtained with a detailed study of the energy spectrum of the electron. The energy spectrum of the ν_e's from oscillations would depend on the value of $\Delta m^2_{e\mu}$ and be different from that of the ν_e from the beam contamination. The increase in sensitivity depends on many factors and has not been quantified yet.

It should be noted that the expected number of "electron" events at the far detector may be estimated using a Monte Carlo simulation rather than measuring it in the detector at the close location. This method has the advantage of extending the sensitivity of the experiment to higher values of Δm^2, although it does require a knowledge of the detection efficiencies for electrons, muons and π°. A complete study is in progress; at this stage, we believe that under reasonable assumptions the systematic error on the electron contamination may be kept at a level of 10%, while that on the π°'s is much larger (we have assumed 50%), owing to the uncertainty on the production cross sections and detection efficiency. The increase in the

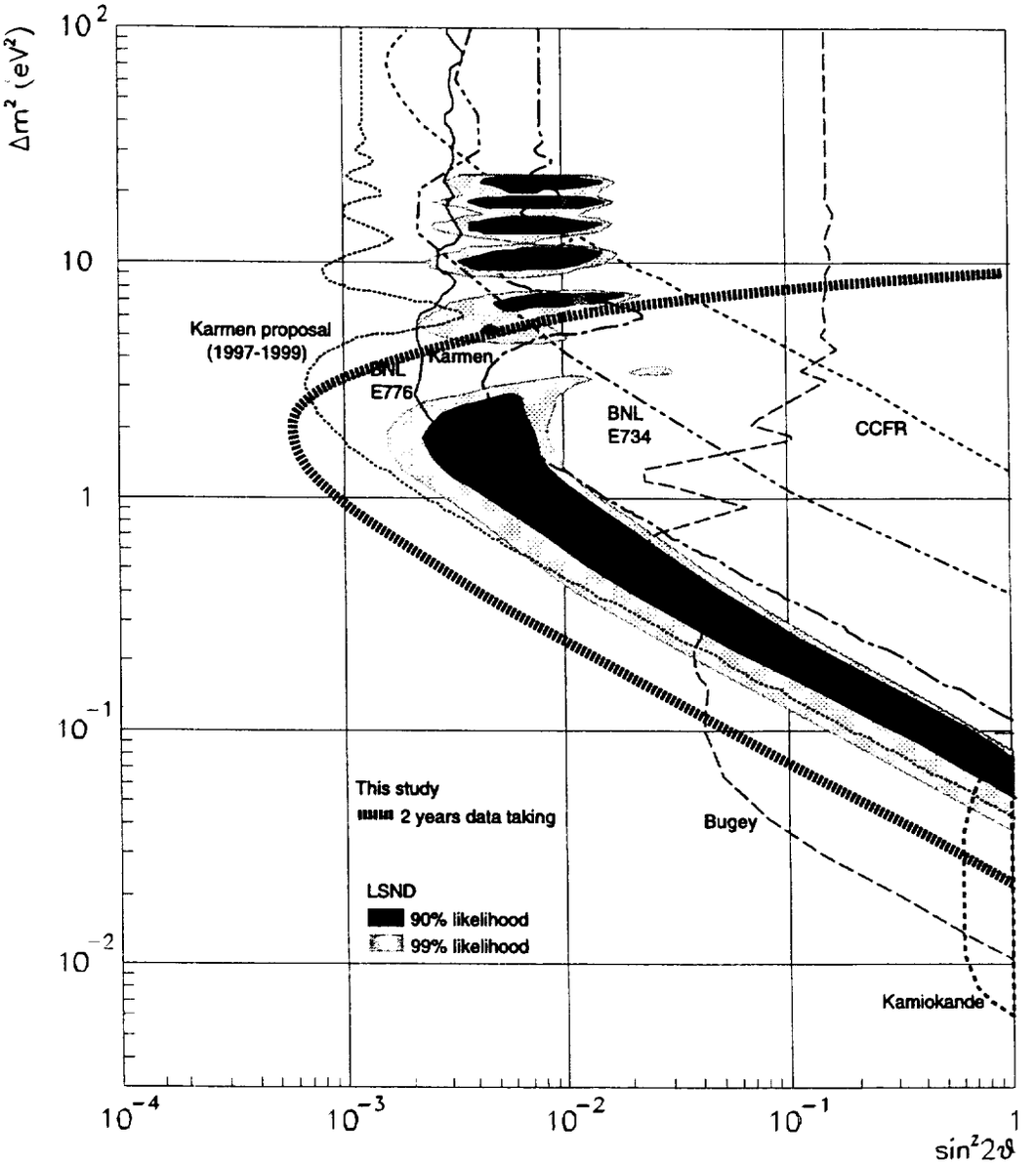

Figure 13: Two detectors $\nu_\mu \rightarrow \nu_e$ exclusion plot.

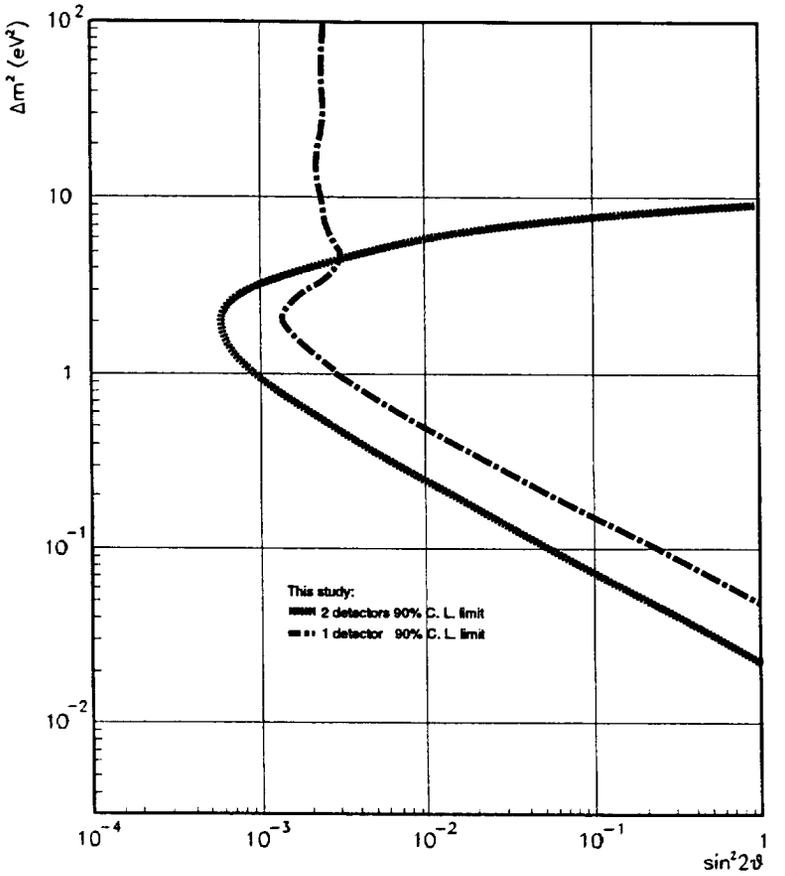

Figure 14: Limit on $\nu_\mu \rightarrow \nu_e$ with one detector. The limit obtained with two detectors is also shown for comparison.

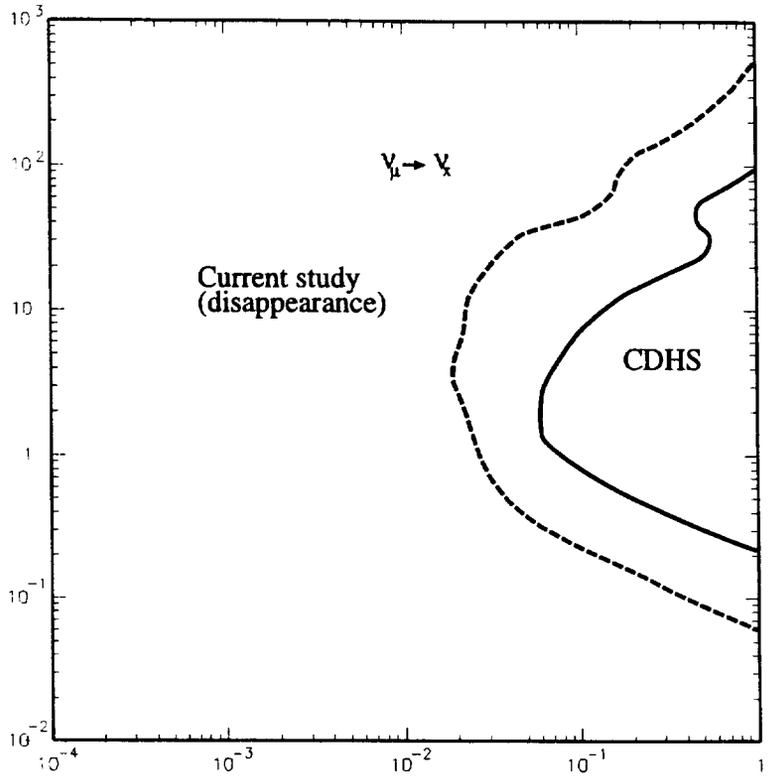

Figure 15: Two detectors $\nu_\mu \rightarrow \nu_x$ exclusion plot (disappearance).

systematic uncertainty appreciably reduces the sensitivity to oscillations, as shown in figure 14. For this reason, we believe that the two-detectors method proposed is far superior.

It should be observed that the detector, in its present design, has an excellent capability to separate electrons from π° and consequently the main contribution to the background comes from the ν_e contamination in the beam. Therefore a reduction of this contamination using techniques such as those described in [25], could, at a later stage, lead to a substantial improvement of the result.

Although it is not the primary objective of this experiment, a test for the disappearance of ν_μ can be performed using the reduced sample of events (about 30% of the total) in which the muon stops in the apparatus and it is possible to measure its momentum from its range and therefore compute the energy of the incoming neutrino. The attainable limits are displayed in figure 15.

7 Summary

We have discussed an experiment to search for $\nu_\mu \rightarrow \nu_e$ oscillations at a distance of about 900 m from a source of neutrinos with about 1.5 GeV average energy. A fine grained calorimeter is used to detect events with an electron in the final state and hence the appearance of ν_e in the CERN PS ν_μ beam. A "close" detector, identical to the "far" detector, is employed to measure all backgrounds, thus making possible a background subtraction in the far detector, practically free from systematic uncertainties.

In summary the salient features of the experiment are:

- its sensitivity to mixing angles as small as $6 \cdot 10^{-4}$ in the $\Delta m^2 \sim 1\ eV^2$ region, which is of interest for cosmology;
- its capability to check with high sensitivity and a different technique the LSND claim for oscillation;
- its time scale, since, using existing technology, it could be operational in a relatively short time. Data taking could take place in the years 2000-2001.

Acknowledgments

We warmly thank R. Cappi and the PS division staff, for the helpful investigation of the possibility of restoring the PS neutrino beam line.

References

[1] C. Athanassopoulos et al., LSND coll., Phys. Rev. C54 (1996) 2685.
C. Athanassopoulos et al., LSND coll., Phys. Rev. Lett. 77 (1996) 3082.

[2] C. Athanassopoulos et al., LSND coll., nucl-ex/9709006.

[3] G. L. Fogli, E. Lisi and D. Montanino, Phys. Rev. D54 (1996) 2048.

[4] S. Bilenky et al., Phys. Rev D, 54 (1996) 1881.

[5] A. Acker and S. Pakvasa, Phys. Lett. B, 397 (1997) 209.

[6] C. Y. Cardall and G. M. Fuller, Phys. Rev. D, 53 (1996) 4421.

[7] M. de Jong et al., CERN-PPE/93-131.

[8] P. Astier et al., CERN-SPSLC/91-21, CERN-SPSLC/91-48// CERN-SPSLC/91-53,CERN-SPSLC/92-51.

[9] W. W. M. Allison, Phys. Lett. B, 391 (1997) 491.

[10] M. Koshiba, Phys. Rep. 220 (1992) 358.

[11] K. Martens, presented at Int. Conf. on HEP, Jerusalem, August 1997, to be published in the conf. proceed.

[12] C. Bemporad, presented at Int. Conf. on HEP, Jerusalem, August 1997, to be published in the conf. proceed.

[13] K. Eitel et al., Proc. of the 8th Rencontres de Blois "Neutrinos, Dark Matter and the Universe", June 1996.

[14] M. Giammarchi, Nucl. Phys. Proc. Suppl. B35 (1994) 433.

[15] G. Ewan et al., Sudbury Neutrino Observatory Proposal, SNO-87-12 (1987).

[16] K. Nishikawa et al., KEK-PS Proposal E362 (1994)

[17] C. Rubbia, ICARUS Coll., Nucl. Phys. Proc. Suppl. B48 (1996)
G. C. Barbarino et al., NoE Coll., INFN-AE-96-11 (1996).
T. Ypsilantis et al., LPC 96-01, CERN-LAA 96-02 (1996).
A. Ereditato et al., DAPNU-97-07, INFN-AE-97-06.

[18] E. Ables et al., FERMILAB proposal P-875 (February 1995).

[19] COSMOS Coll., 1995 Update Report on FERMILAB E803/COSMOS.

[20] A. S. Ayan et al., CERN-SPSC/97-5, SPSC/I 213, March 1997.

[21] E. Church et al., LA-UR-97-2120, June 1997.

[22] M. Bonesini et al., CERN-SPSLC 95-37, SPSLC/I 205.

[23] ICARUS-CERN-Milano Coll., CERN/SPSLC 96-58, SPSLC/P 304 (1996).

[24] J. Primack et al., Proc. of the 17th Int. Conf. on Neutrino Physics and Astrophysics - NEUTRINO96, Helsinki, June 1996 (hep-ph/9610321).

[25] L. Ludovici, P. Zucchelli CERN-PPE/97-181, hep-ph/9701007, subm. to Nucl.Instr. and Meth.

[26] L. Borodovsky et al., Phys.Rev.Lett. 68 (1992) 274.

[27] L. A. Ahrens et al., Phys. Rev. D31 (1985) 2732.

[28] S.Ricciardi, private communication.

[29] C. Angelini et al., Phys.Lett. B179 (1986) 307.

[30] H. Faissner et al., Phys. Lett. B125 (1983) 230.

[31] G. Bernardi et al., Phys.Lett. B166 (1986) 47
P. Astier et al.,Nuclear Physics B335 (1990) 517-545

[32] J. V. Allaby et al., Z. Phys. C40 (1988) 171

[33] F. Dydak et al., Phys. Lett. B134 (1984) 281.

[34] D.Geigerat et al., Nucl.Instr. and Meth. A325 (1993) 92.

[35] CERN program library long writeup Q123, version 3.21, June 1993.

[36] J.V.Allaby et al., CERN/70-12 and reference therein.

[37] R.Cappi, private communication.

[38] K. Lang, UTKL-119, NuMI-L-249.